Click Here for Full Article

Impact of vegetation coverage on regional water balance in the nonhumid regions of China

Dawen Yang,[1] Weiwei Shao,[1] Pat J.-F. Yeh,[2] Hanbo Yang,[1] Shinjiro Kanae,[2] and Taikan Oki[2]

Received 26 February 2008; revised 22 November 2008; accepted 15 December 2008; published 3 March 2009.

[1] The growth of vegetation is affected by water availability, while vegetation growth also feeds back to influence regional water balance. A better understanding of the relationship between vegetation state and water balance would help explain the complicated interactions between climate change, vegetation dynamics, and the water cycle. In the present study, the impact of vegetation coverage on regional water balance was analyzed under the framework of the Budyko hypothesis by using data from 99 catchments in the nonhumid regions of China, including the Inland River basin, the Hai River basin, and the Yellow River basin. The distribution of vegetation coverage on the Budyko curve was analyzed, and it was found that a wetter environment (higher P/E_0) had a higher vegetation coverage (M) and was associated with a higher evapotranspiration efficiency (E/E_0). Moreover, vegetation coverage was related not only to climate conditions (measured by the dryness index $DI = E_0/P$) but also to landscape conditions (measured by the parameter n in the coupled water–energy balance equation). This suggests that the regional long-term water balance should not vary along a single Budyko curve; instead, it should form a group of Budyko curves owing to the interactions between vegetation, climate, and water cycle. A positive correlation was found between water balance component (E/P) and vegetation coverage (M) for most of the Yellow River basin and for the Inland River basin, while a negative correlation of $M \sim E/P$ was found in the Hai River basin. Vegetation coverage was successfully incorporated into an empirical equation for estimating the catchment landscape parameter n in the coupled water–energy balance equation. It was found that interannual variability in vegetation coverage could improve the estimation of the interannual variability in regional water balance.

Citation: Yang, D., W. Shao, P. J.-F. Yeh, H. Yang, S. Kanae, and T. Oki (2009), Impact of vegetation coverage on regional water balance in the nonhumid regions of China, *Water Resour. Res.*, *45*, W00A14, doi:10.1029/2008WR006948.

1. Introduction

[2] The mechanism of the interactions between the atmosphere, vegetation, and the water cycle in arid or semiarid regions is one of the most widely discussed issues in watershed ecohydrology. Both climate and soil control vegetation dynamics, whereas vegetation exerts a significant influence on regional water balance and feeds back to the atmosphere [*Rodríguez-Iturbe and Porporato*, 2004]. In water-limited environments, vegetation dynamics largely depend on the water availability that results from the complex mutual interactions between climate and hydrological processes [*Rodríguez-Iturbe et al.*, 2001; *Laio et al.*, 2001; *Zeng et al.*, 2005]. The growth of vegetation is affected by intermittent water availability [*Baudena et al.*, 2007], which at the same time influences soil moisture through canopy interception and transpiration [*Eagleson*, 2002].

1.1. Characterizing Vegetation Impact on the Regional Water Balance

[3] *Budyko* [1974] postulates that the primary factors controlling the rate of long-term average evapotranspiration (E) are the availability of energy and water. Usually, the potential evaporation (E_0) is used to measure the availability of energy, while precipitation (P) is used to measure the availability of water. According to the Budyko hypothesis, the actual evapotranspiration in humid regions is mainly controlled by potential evaporation, while in nonhumid regions it is controlled by precipitation. This coupled water–energy balance model is termed the Budyko curve, and is calculated as such [*Budyko*, 1974]:

$$E = P\sqrt{\frac{E_0}{P}\tanh\left(\frac{P}{E_0}\right)\left[1-\exp\left(-\frac{E_0}{P}\right)\right]}. \quad (1)$$

Several previous studies have developed various but somewhat similar coupled water–energy balance equations on the basis of the Budyko hypothesis [e.g., *Zhang et al.*,

[1]State Key Laboratory of Hydro-Science and Engineering, Department of Hydraulic Engineering, Tsinghua University, Beijing, China.
[2]Institute of Industrial Science, University of Tokyo, Tokyo, Japan.

Copyright 2009 by the American Geophysical Union.
0043-1397/09/2008WR006948$09.00

1999, 2001, 2004; *Potter et al.*, 2005; *Yang et al.*, 2006, 2007; *Yang et al.*, 2008a]. These equations are developed empirically or theoretically from different catchments worldwide; and therefore, their formulations are likely influenced by both the specific climate conditions and the landscape characteristics of the specific catchments, although all of the equations show a curve similar to the Budyko curve [*Yang et al.*, 2006]. However, most of these models do not explicitly account for vegetation characteristics, and the impact of vegetation change on the catchment-scale long-term water balance has received little attention (except in work by *Zhang et al.* [1999, 2001]). A number of paired-catchment experiments have shown that evapotranspiration is favored over runoff in forested catchments because of a higher rainfall interception and a more efficient use of soil moisture reserves during growing seasons [*Cosandey et al.*, 2005]. *Donohue et al.* [2007] argue that it was necessary to explicitly include vegetation dynamics into the Budyko curve particularly at small spatial ($\leq$1000 km^2) and temporal scales ($\leq$1 to 5 years). Donohue et al. further suggest that some key vegetation attributes, including leaf area, photosynthetic capacity, and rooting depth, may exert significant influences on the coupled water and energy balance of a catchment.

[4] *Choudhury* [1999] develops the following empirical equation of annual evaporation on the basis of the earlier work by *Pike* [1964]:

$$E = P/[1 + (P/R_n)^{\alpha}]^{1/\alpha}, \tag{2}$$

where R_n is the water equivalent of annual net radiation and α is an adjustable parameter. The parameter α is evaluated as 2.6 from field observations at eight locations with different vegetation types, and as 1.8 from the results of a biophysical process–based model in ten river basins. On the basis of dimensional analysis and mathematical reasoning, *Yang et al.* [2008a] derive an analytical equation of the coupled water–energy balance at an annual time scale, which has a similar form to equation (2):

$$E = \frac{E_0 P}{\left(P^n + E_0^n\right)^{1/n}}, \tag{3}$$

where the parameter n reflects the catchment landscape characteristics. This theoretical equation has also been extended to a variety of time scales. On the basis of field measurements in a winter wheat farmland, *Yang et al.* [2008b] find a clear linear correlation between n and LAI (leaf area index) at the 10-day time scale, which implies the possibility of correlating vegetation characteristics with the coupled water–energy balance model.

[5] *Zhang et al.* [1999, 2001] propose the following simple two-parameter model on the basis of the Budyko hypothesis:

$$E = P\left(f\frac{1 + w_1 \times E_0/P}{1 + w_1 \times E_0/P + P/E_0} + (1-f) \cdot \frac{1 + w_2 \times E_0/P}{1 + w_2 \times E_0/P + P/E_0}\right), \tag{4}$$

where f is the fractional forest cover, and w_1 and w_2 are the plant-available water coefficients for forest and nonforest (i.e., herbaceous vegetation) areas, respectively. In the original global model of *Zhang et al.* [2001], the values of w_1 and w_2 are set equal to 2.0 for forest areas and 0.5 for nonforest areas, and the model agrees well with data from 250 catchments worldwide. *McVicar et al.* [2007] improve the value of the model parameters by incorporating the results from local field studies. McVicar et al. apply the new model to the Loess Plateau in China to simulate the regional impacts of forestation on average annual stream flow. By using the model of *Zhang et al* [2001], *Oudin et al.* [2008] incorporate vegetation information (i.e., area fraction of the vegetation cover) on the basis of a global data set into different types of Budyko curves to investigate the vegetation's impact on the long-term average stream flow. Their results show that land cover information has a significant contribution to the improvement of model efficiency.

[6] Moreover, vegetation coverage and vegetation type are mainly controlled by both water availability and solar radiation intensity. *Bonan* [2002] summarizes the distribution of major plant formations, such as the tropical rainforest and the temperate forest, on the basis of the zones of mean annual temperature and precipitation. *Holdridge* [1967] depicts plant life zones as hexagons formed by the intersection of mean annual biotemperature and annual precipitation. Consequently, it is reasonable to expect that certain internal relationships may exist between the vegetation characteristics and the coupled water–energy balance; this calls for further research.

1.2. Ecosystem Degradation Problem in the Nonhumid Regions of China

[7] In recent decades, water shortage and soil erosion due to deforestation, overcultivation and intensive water resources development, have been the main ecosystem degradation problems in the nonhumid regions of northern China [*Jiao et al.*, 2007; *Chen et al.*, 2007]. The Yellow River has periodically dried up along its lower reaches during the irrigation season since 1972, and this situation intensified in the 1990s. The decrease in river discharge has likewise caused a rapid rise of the riverbed of the lower reaches of the Yellow River because of heavy erosion in the Loess Plateau and sedimentation along the lower reaches [*Yang et al.*, 2004]. Though the soil erosion problems in the Hai River and the Inland River basin are not as severe as in the Yellow River basin, intensive development of water resources has resulted in no water being discharged into the sea or into downstream lakes.

[8] In 1998, the Chinese government initiated the Nature Forest Protection Project (NFPP) to prevent severe soil erosion and to ensure sustainable development [*McVicar et al.*, 2007]. The Loess Plateau, which is located in the middle reaches of the Yellow River basin, is one of the "hot spots" of environmental degradation, with erosion rates ranging from 20,000 to 30,000 tons km^{-2} a^{-2} [*Xu et al.*, 2004]. Hence, in 1999 the Chinese government mandated that forest cover should be significantly increased in the Loess Plateau [*Zhang et al.*, 2007]. Future forestation practices should consider the complex impacts of vegetation coverage on regional water balance in water-limited areas, otherwise additional environmental problems may emerge.

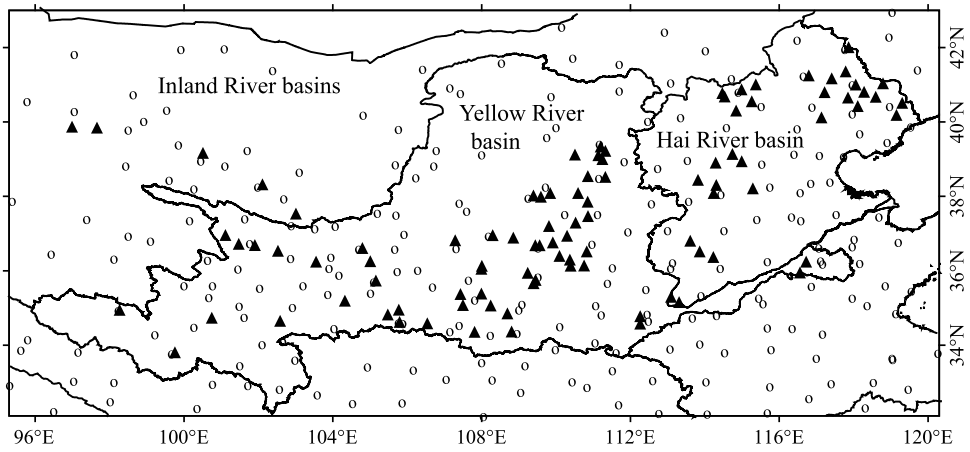

Figure 1. Study areas in nonhumid regions of China, including the Inland River basin, the Hai River basin, and the Yellow River basin. The triangles represent location of the 99 hydrological stations at catchment outlets, and the circles represent locations of the 238 meteorological stations.

Unconstrained forestation practices may lead to excessive soil moisture depletion and the development of a dry soil layer such that there will not be sufficient water available to maintain normal growth rates in the revegetated areas [*McVicar et al.*, 2007]. Understanding the interactions between the atmosphere, vegetation, and water cycle in nonhumid regions is required to derive a guideline for the effective forestation practices and for soil and water conservation in northern China.

1.3. Objectives of This Study

[9] The objective of this study was to explore the relationships between vegetation coverage and regional water balance, believed to be useful in predicting the ecohydrological responses of a water-limited environment to climate changes and to human activities. In the following sections, the impact of vegetation on long-term regional water balance was investigated under the framework of the Budyko hypothesis by using data from 99 catchments in the nonhumid regions of China. An attempt was also made to incorporate vegetation characteristics into the regional water balance model, primarily for the purpose of improving the estimation of the interannual variability of evapotranspiration.

2. Study Area and Data

[10] The 99 catchments in the nonhumid regions of China were selected as the study areas in this study (see Figure 1), and included 62 catchments in the Yellow River basin, 30 catchments in the Hai River basin, and 7 catchments in the Inland River basin. Among the 62 catchments in the Yellow River basin, 51 were located in the Loess Plateau region, nine in the Tibetan Plateau region, and two in the lower reaches of the Yellow River basin. All 99 catchments had relatively minor human interferences, such as dam operation and irrigation diversion. Table 1 summarizes the primary basin characteristics and the long-term average water balances of the 99 study catchments.

[11] Long-term meteorological data from a total of 238 meteorological stations within the study area were provided by the China Administration of Meteorology (see Figure 1 for their locations). The data consist of daily precipitation, air temperature, sunshine duration, wind speed, and relative humidity from 1956 to 2005. Additionally, daily solar radiation data for 47 of the 238 meteorological stations were available for the calculation of potential evaporation in this study. In addition, the Hydrological Bureau of the Ministry of Water Resources of China provided the 1951–2000 monthly stream discharge data at the outlets of the 99 catchments [*Yang et al.*, 2006]. By assuming that the annual change of water storage was zero, the annual evapotranspiration from 1956 to 2000 for each catchment was calculated by subtracting the annual discharge from the annual precipitation [*Yang et al.*, 2007].

[12] The catchment boundary was extracted by using the 1-km DEM (digital elevation model) for the estimation of area-averaged hydroclimatic variables. The procedures for calculating catchment average precipitation and potential evaporation include the following: (1) a 10-km gridded data set covering the study area was interpolated from the station data by using the distance-direction-weighted average method, except that the interpolation of temperature was modified with the altitude; (2) daily potential evaporation was estimated for each grid by using the Penman equation following *Shuttleworth* [1993]; and (3) the catchment average values were then calculated for each variable (see *Yang et al.* [2004] for details). For the estimation of net radiation, solar radiation was calculated by using an empirical equation involving daily sunshine duration [*Yang et al.*, 2006]. The first-order estimate of net long-wave radiation was derived from the relative sunshine duration, surface minimum and maximum air temperature, and vapor pressure, following the method recommended by FAO [*Allen et al.*, 1998].

[13] A global data set of monthly normalized difference vegetation index (NDVI) from 1982 to 2000 with 1-km resolution was obtained from the NOAA advanced very high resolution radiometer (AVHRR). Monthly vegetation coverage was calculated from the NDVI data by using the method proposed by *Gutman and Ignatov* [1998]:

$$M = (NDVI - NDVI_{\min})/(NDVI_{\max} - NDVI_{\min}), \quad (5)$$

Table 1. Basin Characteristics and Long-Term Average Precipitation, Actual Evapotranspiration, Potential Evaporation, and Vegetation Coverage of the 99 Study Catchments Shown in Figure 1[a]

Code	Area (km^2)	Mean Values (mm a^{-1}) $\overline{P}$	$\overline{E}$	$\overline{E_0}$	M	n
		Inland River Basin				
4010	10961	179	100	966	0.11	0.6
4071	800	195	162	1026	0.09	1.0
4087	14325	152	127	1036	0.04	0.9
4147	11388	247	155	1011	0.21	0.7
4215	2240	275	199	886	0.24	0.9
4403	877	301	235	947	0.33	1.1
4455	2053	247	182	965	0.20	0.9
		Hai River Basin				
31261	1378	473	413	898	0.43	1.9
31271	1025	678	555	867	0.49	2.3
31272	1166	753	635	844	0.51	3.1
31353	1227	447	409	831	0.39	2.4
31428	1615	572	496	869	0.45	2.3
31453	2404	466	426	870	0.43	2.4
31464	2220	521	433	866	0.34	1.8
31507	1661	639	534	865	0.42	2.3
31531	2822	705	584	865	0.41	2.5
31551	372	577	506	848	0.36	2.5
31663	5060	705	588	888	0.41	2.5
32152	2950	634	544	931	0.46	2.3
32352	1927	497	452	892	0.42	2.4
32353	4700	490	441	921	0.44	2.2
33456	3674	367	357	956	0.25	2.7
33458	2890	414	395	969	0.24	2.5
33464	272	419	370	839	0.37	1.9
33467	2360	414	392	892	0.31	2.5
33552	25533	454	446	959	0.24	3.6
33600	15078	385	370	964	0.24	2.4
34451	2950	648	586	976	0.34	2.8
34452	4990	648	598	1009	0.34	3.0
34471	4061	572	518	1025	0.36	2.3
35251	14070	502	471	974	0.34	2.6
35262	5387	516	483	1009	0.34	2.6
35263	6420	509	460	1070	0.36	2.0
35271	23900	564	545	1068	0.41	3.3
36252	3800	570	532	888	0.43	3.2
36253	5060	563	512	866	0.35	2.8
36255	19050	514	492	893	0.27	3.3
		Yellow River Basin				
41000	20930	321	279	879	0.19	1.5
41002	45019	443	367	876	0.24	1.6
41005	98414	577	397	896	0.40	1.2
42202	715	397	330	1032	0.36	1.3
42212	3083	512	419	859	0.22	1.7
42218	9022	512	411	850	0.33	1.6
42222	12573	500	403	1017	0.28	1.4
42582	5043	631	436	789	0.42	1.5
42728	4007	323	297	839	0.25	1.9
42753	990	404	394	886	0.14	3.1
42760	4853	378	368	867	0.12	3.0
42766	10647	375	365	837	0.13	3.1
44003	2831	382	349	929	0.11	1.9
44018	1562	410	400	892	0.21	3.3
44037	1263	381	333	931	0.12	1.6
44039	2939	433	425	886	0.28	3.6
44063	650	445	395	899	0.42	1.9
44071	3829	340	299	958	0.12	1.5
44077	8645	408	352	967	0.12	1.6
44091	1121	391	350	969	0.11	1.7
44099	283	426	386	982	0.24	1.9
44115	4102	428	388	934	0.39	2.0
44143	15325	331	306	988	0.10	1.8
44153	29662	366	332	963	0.12	1.7
44161	2415	371	349	886	0.11	2.3
44167	327	386	348	918	0.08	1.8
44201	913	420	378	873	0.12	2.0
44203	3468	438	395	897	0.14	2.0
44227	3992	449	426	875	0.35	2.7
44235	5891	457	422	870	0.22	2.4
44243	3208	420	378	867	0.15	2.0
44244	719	446	409	856	0.29	2.3
44253	1121	487	471	871	0.41	3.6
44254	1662	474	455	888	0.26	3.1
44259	2169	511	489	877	0.47	3.5
44261	436	468	447	887	0.41	3.0
45502	3440	395	364	858	0.12	2.2
45504	774	421	382	840	0.15	2.1
45511	17180	555	528	879	0.35	3.4
45546	4715	495	473	829	0.47	3.6
45562	2266	549	509	841	0.50	3.1
46005	600	465	426	751	0.32	2.8
46024	4788	487	467	936	0.34	3.1
46037	37006	625	559	899	0.48	2.8
46043	46827	675	601	810	0.45	3.6
46069	2484	448	432	929	0.19	2.9
46085	9805	410	394	914	0.25	2.7
46125	1019	470	426	922	0.33	2.1
46288	282	558	516	812	0.41	3.3
46517	14124	491	452	841	0.37	2.6
46520	40281	509	477	859	0.26	3.0
46571	4640	372	353	967	0.12	2.2
46591	10603	446	421	908	0.16	2.6
46593	2988	416	386	862	0.21	2.3
46597	19019	494	468	850	0.33	3.1
46623	928	488	449	949	0.38	2.3
47209	9713	824	674	871	0.37	3.1
47275	829	585	500	1219	0.37	1.6
47320	12880	594	555	971	0.43	3.1
47373	3149	552	512	849	0.35	3.1
48029	8264	709	625	1009	0.39	2.7
48066	426	624	565	1023	0.36	2.5

[a]Average precipitation is for 1982 to 2000. Vegetation coverage is in percent.

where M is the vegetation coverage, which represents the fraction of total ground surface covered by vegetation, dimensionless. $NDVI_{min}$ and $NDVI_{max}$ are the NDVI signals from bare soil and dense green vegetation respectively. Gutman and Ignatov propose $NDVI_{min}$ and $NDVI_{max}$ as global constants independent of vegetation/soil type. In our study, we prescribe the $NDVI_{min} = 0.05$ and $NDVI_{max} = 0.80$ respectively according to some references [*Montandon and Small*, 2008; *Steven et al.*, 2003; *Carlson and Ripley*, 1997]. The vegetation coverage calculated has a linear relationship with the NDVI data, and indicates the fraction of the green vegetation in the region.

[14] For the purpose of comparison, the land use map with 1-km resolution for northern China (including Qinghai, Ningxia Shaanxi, Gansu, Hebei, Liaoning provinces and the city of Beijing) was obtained from the Chinese Academy of Sciences (CAS) [*Liu et al.*, 2002] and the land use/cover was classified into the following six types: rain-fed cropland, forest land, grassland, water body, built-up land, and unused land.

[15] The long-term (1982–2000) average water balance (precipitation, actual and potential evapotranspiration) and the vegetation data for the 99 catchments are summarized in Table 1. The annual precipitation, actual evapotranspiration, potential evaporation and vegetation coverage percentage

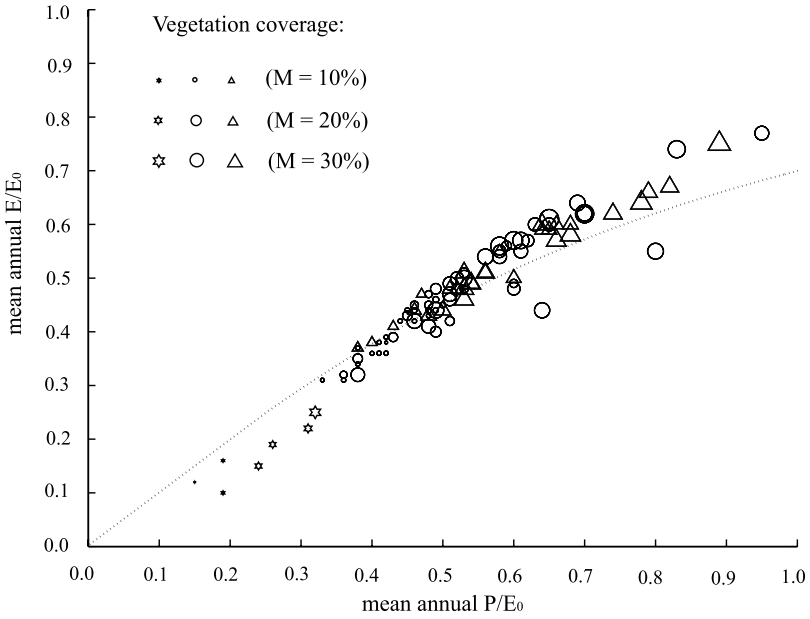

Figure 2. Distribution of vegetation coverage on the Budyko curve by using the data from the 99 catchments in the nonhumid regions of China. The Budyko curve calculated by equation (1) is plotted as a dotted line. The stars represent the catchments in the Inland River basin; the triangles represent the catchments in the Hai River basin; and the circles represent the catchments in the Yellow River basin.

are, respectively, 228 mm, 166 mm, 977 mm, and 17% for the Inland River basin; 541 mm, 485 mm, 920 mm, and 37% for the Hai River basin; and 469 mm, 424 mm, 901 mm, and 27% for the Yellow River basin. The values are averaged among the 7 catchments in the Inland River basin, 30 catchments in the Hai River basin and 62 catchments in the Yellow River basin in the period from 1982 to 2000, respectively.

3. Analyzing Vegetation Impacts on Regional Water Balance by Using the Budyko Curve

3.1. Distribution of Vegetation Coverage on the Budyko Curve

[16] The long-term average annual precipitation, potential evaporation and actual evapotranspiration for the 99 study catchments have been used by *Yang et al.* [2006, 2007] for the validation of the Budyko curve, and have shown that the change in actual evapotranspiration in a nonhumid region is controlled mainly by the change in precipitation, rather than by potential evaporation. In order to investigate the impact of vegetation on regional water balance, the distribution of vegetation on the Budyko curve is plotted in Figure 2 by using data from the 99 study catchments during the period of 1982 to 2000, including the long-term average annual precipitation, potential evaporation, actual evapotranspiration and vegetation coverage (Table 1). The size of the plotting symbol (see Figure 2) was proportional to the average annual vegetation coverage (M) of the catchment. Since all 99 catchments were located in the nonhumid regions of China with annual precipitation ranging from 152 to 824 mm, actual evapotranspiration was controlled mainly by the water availability. As shown in Figure 2, M had a clear linear relationship with annual precipitation following the trajectory of the Budyko curve, indicating that the long-term regional annual water balance was sensitive to M. For a dryer catchment, both the evapotranspiration efficiency (E/E_0) and M were lower, while they were higher for a wetter catchment.

[17] There were 74 catchments over the study area where detailed land use maps were available. Of these 74, 48 catchments were located in the Yellow River basin, 19 in the Hai River basin, and seven in the Inland River basin. The majority of the catchments in the Yellow River basin and the Hai River, and all the catchments in the Inland River basin have the land use data. The average annual vegetation coverage derived from the NDVI is about 39% for the 19 catchments of the Hai River basin and 25% for the 48 catchments of the Yellow River basin. The comparison between the land use map and the average annual vegetation coverage derived from the NDVI in the 74 catchments is listed in Table 2. On the basis of detailed land use maps, the forest area fraction in the Inland River basin, Hai River basin, and Yellow River basin was 12%, 52%, and 13%, respectively; however the density of forest is different in the three basins. The density of forest and grass is relatively higher in the Hai River basin than in the Yellow River basin and the Inland River basin. The average forest area fraction in the Hai River basin was significantly higher than those in the other two basins. The 74 catchments in northern China can be divided into three groups according to the forest area fraction F: $\geq$25%, between 10% and 25%, and $\leq$10%, respectively, with each containing a nearly equal number of catchments. From this classification it was found that F was significantly correlated with total vegetation coverage (M), and each group exhibited a distinct range on the Budyko curves (Figure 3). Figure 3 also shows the distribution of both M and F on the Budyko curve by using data from the 74 catchments. It can be seen that the distribution of F on the Budyko curve follows a similar pattern to that of M.

Table 2. Comparison Between the Land Use Map and the Average Annual Vegetation Coverage Derived From the NDVI in the 74 Catchments of the Nonhumid Region

		Land Use Type and Area Percentages[a]				
Average Value	Vegetation Coverage From NDVI M (%)	Forest Land (%)	Grassland (%)	Rain-Fed Cropland (%)	Other Land Use (%)	Correlation Between M and Forest Land Proportion
Inland River basin	17	12	43	6	39	0.96
Hai River basin	39	52	25	21	3	0.68
Yellow River basin	25	13	45	32	10	0.80

[a]The density of forest and grass in each basin is different, which is relatively higher in the Hai River basin than in the Yellow River basin and the Inland River basin.

[18] The correlation coefficients between M and the ratios P/E_0, E/E_0, and E/P are summarized in Table 3, from which it can be seen that vegetation coverage M has a clear positive correlation with both P/E_0 and E/E_0. The ratio P/E_0 denotes the degree of climate wetness, while E/E_0 represents the evaporation efficiency. It can be concluded that for a wetter environment, both M and E/E_0 are higher. This is consistent with the findings presented in most of the previous paired catchment studies [*Brown et al.*, 2005; *Zhang et al.*, 1999], which show that for two catchments with a similar climate (P and E_0) and landscape characteristics, the catchment with more vegetation tended to have higher evapotranspiration. This is mainly due to increases in transpiration as well as interception from leaves and stems, and more infiltration resulting from the better soil conditions developed by vegetation.

[19] Figure 4 shows the distribution of vegetation coverage (M) and forest area percentage (F) on the alternative Budyko curve, that is, the plot of E/P versus E_0/P rather than the original Budyko curve: E/E_0 versus P/E_0. By comparing Figures 2 and 3, it is seen that the change in actual evapotranspiration was controlled by the change in precipitation rather than by potential evaporation. Figure 4 shows that vegetation coverage was different given the dryness index ($DI = E_0/P$), which is due to the difference in landscape characteristics.

[20] Table 4 summarizes the regional differences in the dryness index and the long-term average annual vegetation coverage in the three study basins. As shown in Table 4, with a narrow range in the dryness index, the Hai River basin consistently has higher vegetation coverage than the Yellow River basin. The average annual dryness index (DI) for the Hai River basin ($DI = 1.70$) was similar to that in the Yellow River basin ($DI = 1.92$); however, the average annual vegetation coverage in the Hai River basin ($M = 37\%$) was much higher than it was in the Yellow River basin ($M = 27\%$). On one hand, the major soil type in the Hai River basin is a loam (brunisolic soil and drab soil), while in the Yellow River basin coarse sand and gravel predominate, which results in the soil with a lower water-holding capacity than that in the Hai River basin (Food and Agriculture Organization of the U. N., Map of soil texture of China,

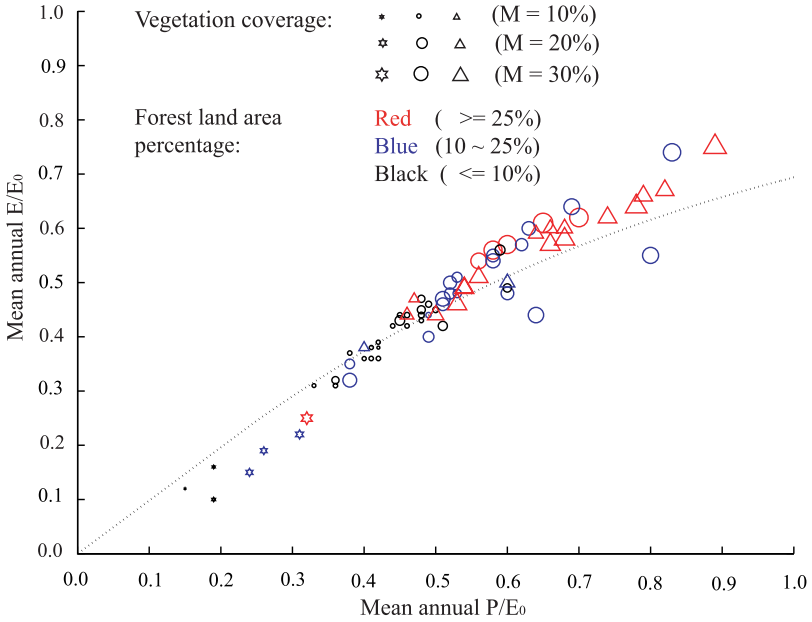

Figure 3. Distribution of vegetation coverage and forest land area percentage on the Budyko curve by using data from 74 catchments in the nonhumid regions of China. The Budyko curve calculated by equation (1) is plotted as a dotted line. The stars represent the catchments in the Inland River basin; the triangles represent the catchments in the Hai River basin; and the circles represent the catchments in the Yellow River basin.

Table 3. The Correlation Coefficient Among Vegetation Coverage M, P/E_0, E/E_0, and E/P for the 99 Study Catchments[a]

Region[b]	Correlation Coefficient R		
	$M \sim P/E_0$	$M \sim E/E_0$	$M \sim E/P$
The whole study area (1.1∼6.8)	0.71	0.69	−0.01
The Inland River basin (3.1∼6.8)	0.96	0.86	−0.13
The Hai River basin (1.1∼2.6)	0.68	0.63	−0.70
The Yellow River basin (1.1∼3.1)	0.69	0.69	−0.16

[a]The correlation of $M \sim P/E_0$ and $M \sim E/E_0$ passes the F test with significance level of 1% for all three regions. The correlation of $M \sim E/P$ passes the significance test with significance level of 1% for the Hai River basin, while the negative correlation is not significant for the Inland River basin and the Yellow River basin.
[b]Dryness index is given in parentheses.

http://www.fao.org/WAICENT/FAOINFO/AGRICULT/AGL/swlwpnr/reports/y_ea/z_cn/home.htm). On the other hand, the vegetation in an individual basin appeared to have its own adaptive strategy to the arid climate through the long-term natural selection, which is determined by the combined contribution of precipitation characteristics, soil properties, nutrient availability, and other climate factors [*Eagleson*, 2002]. This was supported by observing that when the dryness index was high (3 to 3.5), vegetation coverage in the Inland River basin, which is the driest among three basins, was still higher than in the other two basins. Moreover, most of the vegetation in the Inland River basin was the drought-tolerant plants species such as *Tamarix chinensis* and *Nitraria tangutorum* [*Xu et al.*, 2007].

3.2. Discussion of the Interaction Between the Atmosphere, Vegetation, and the Water Cycle

[21] Figure 5 shows the statistical relationship between the dryness index and land cover types for the 74 catchments where the detailed vegetation classification data were available. It can be seen that total vegetation area percentage (including forest land, grassland, and rain-fed cropland) decreased when the dryness index increased over these regions; whereas the forest land area percentage decreased sharply when the dryness index increased from less than 1.5 to 2.5, and that forest land area percentage remained almost at the same value (about 10%) when the dryness index was larger than 3.0. Inversely, the percentage of grassland area increased as the dryness index increased from less than 1.5 to 2 and then remained constant, at about 40% as the dryness index further increased. It can be inferred that when the catchment dries up, the forest gradually dies, whereas the grassland survives owing to its seasonal characteristics.

[22] As mentioned above, the variability of actual evapotranspiration in the nonhumid regions is controlled mainly by precipitation variability rather than by potential evaporation. Therefore, as shown in Figures 2 and 3, the evaporation efficiency (E/E_0) exhibited a significant positive correlation with the ratio of P/E_0 (also see Table 3). Because

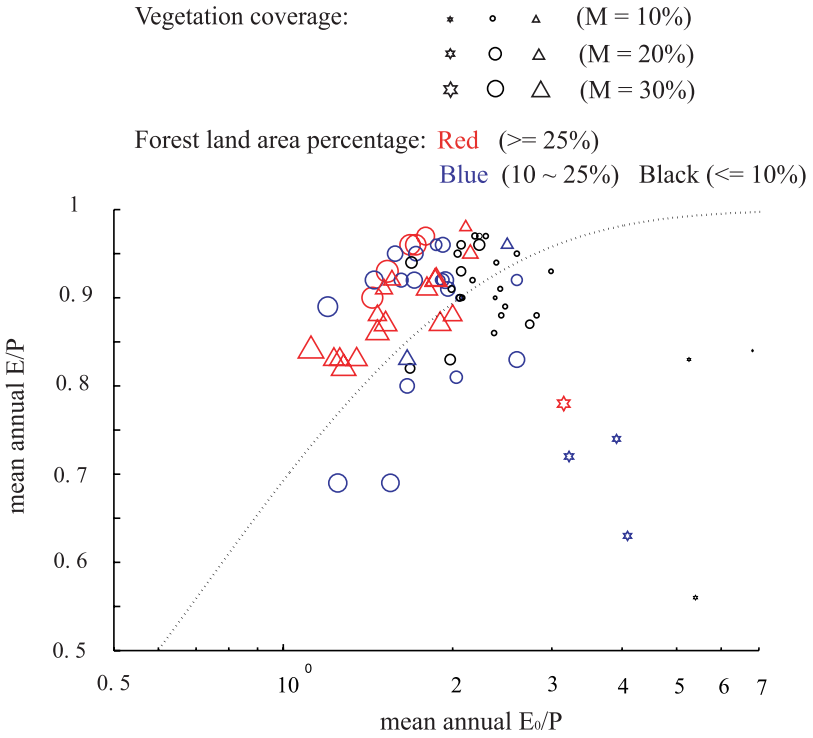

Figure 4. Distribution of the vegetation coverage and forest land area percentage on the alternative Budyko curve (i.e., E/P versus E_0/P) by using data from 74 catchments in the nonhumid regions of China. The Budyko curve calculated by equation (1) is plotted as a dotted line. The stars represent the catchments in the Inland River basin; the triangles represent the catchments in the Hai River basin; and the circles represent the catchments in the Yellow River basin.

Table 4. Regional Differences in the Dryness Index E_0/P and in Vegetation Coverage M Among the Three River Basins

	Dryness Index								
	6.5∼7	5∼5.5	4∼4.5	3.5∼4	3∼3.5	2.5∼3	2∼2.5	1.5∼2	1∼1.5
Inland River Basin									
Mean annual M	0.04	0.10	0.21	0.20	0.28	-	-	-	-
Percentage of catchments	14	29	14	14	29	-	-	-	-
Hai River Basin									
Mean annual M	-	-	-	-	-	0.24	0.30	0.38	0.43
Percentage of catchments	-	-	-	-	-	7	17	53	23
Yellow River Basin									
Mean annual M	-	-	-	-	0.10	0.18	0.20	0.36	0.42
Percentage of catchments	-	-	-	-	2	11	42	37	8

the actual evapotranspiration consisted of mainly vegetation transpiration, E/E_0 should have a strong positive correlation with M. The significant positive correlation between M and P/E_0 is a result of the significant positive correlation between E/E_0 and P/E_0.

[23] As shown in Table 3, although there was no significant correlation between M and E/P for the Yellow River basin and the Inland River basin, a significant negative correlation was found in the Hai River basin. It is interesting to explore the reasons behind this regional difference. The ratio of E/P was determined by both climate and landscape conditions. The climate condition can be measured largely by the dryness index (i.e., along the horizontal axis in Figure 4), and the landscape condition includes mainly the vegetation coverage, topography, and soil condition (i.e., along the vertical axis in Figure 4). Therefore, E/P depends not only on M or DI, but for certain ranges of DI in the same region with similar landscape parameter n, the ratio of E/P should have a stronger correlation with M. As shown in Table 5, both the DI and n in the Hai River basin varied the least among the three study basins. This might be the reason for a relatively significant correlation between M and E/P in the Hai River basin.

[24] As discussed by *Yang et al.* [2008b], the parameter n in equation (3) represents the effect of the catchment landscape characteristics, such as vegetation, soil properties, and slope gradient. As shown in Figure 6, only when the dryness index was extremely low or extremely high (when the curves approach their two asymptotes independent of n values), the impact of landscape conditions (n) on E/P was small. E/P was close to 1.0 in the extreme dry conditions and to zero in the extreme wet conditions, and both cases had no relation to the landscape conditions. This implies that the regional water balance under extremely dry or extremely wet conditions was controlled by the climate conditions and was independent of landscape conditions. The normal climate n strongly affected the Budyko curves as shown in Figure 6. At the same time, vegetation coverage should have also been related to climate conditions. Therefore, it was observed that vegetation coverage varied with both catchment landscape conditions (n) in the vertical axis direction of Figures 4 and 6 and climate conditions in the horizontal axis direction in Figures 4 and 6. Under normal climate conditions the interaction between vegetation coverage and water balance (represented by E/P) should be investigated on a set of the Budyko curves, instead of on

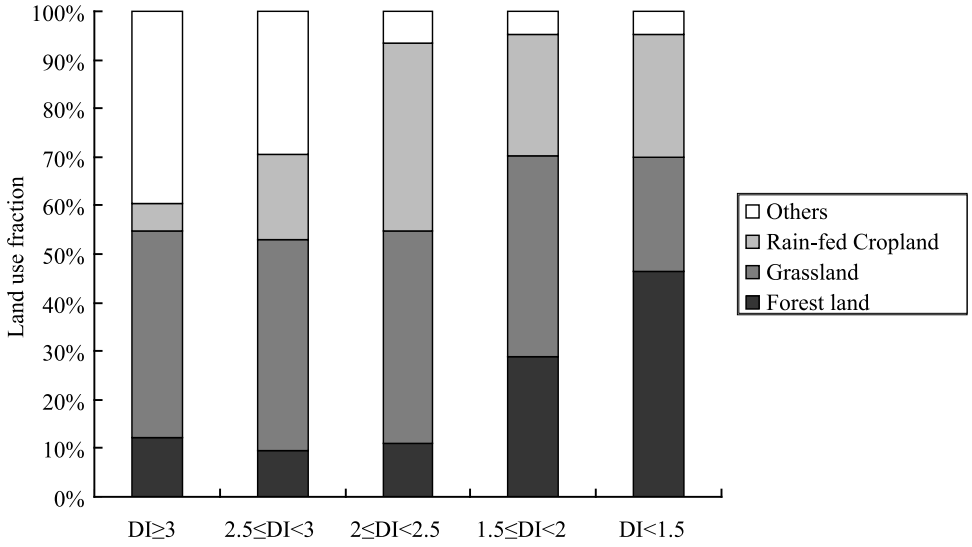

Figure 5. Relationship between dryness index (DI) and land use type and percentages in the 74 catchments of the nonhumid regions of China.

Table 5. Variation of the Parameter n in the Yellow River Basin, the Hai River Basin, and the Inland River Basin

Region[a]	Parameter n		
	Maximum	Minimum	Covariance C_v
The Inland River basin (3.1∼6.8)	1.1	0.6	0.32
The Hai River basin (1.1∼2.6)	3.6	1.8	0.17
The Yellow River basin (1.1∼3.1)	3.6	1.2	0.29

[a]Dryness index is given in parentheses.

Table 6. Relationship Between M and E/P in the 99 Catchments Using Data From 1982 to 2000

Number of Catchments[a]	Significant Positive Correlation ($R > 0.3$)	Significant Negative Correlation ($R < -0.3$)	Nonsignificant Correlation
The whole study area (1.1∼6.8)	19	23	57
The Inland River basin (3.1∼6.8)	1	1	5
The Hai River basin (1.1∼2.6)	1	13	16
The Yellow River basin (1.1∼3.1)	17	9	36

[a]Dryness index is given in parentheses.

only one single curve in order to consider the effects of both landscape conditions and climate.

[25] In order to investigate the behavior of the climate–vegetation–water cycle interactions in different catchments, the 1982–2000 data of the 99 catchments have been analyzed individually. The results presented in Table 6 shows that there was a significant positive correlation between M and for 19 catchments, a significant negative correlation for 23 catchments, and no significant correlation for 57 catchments. The significant positive correlation of $M \sim E/P$ was found mainly in the semiarid regions, including the Inland River basin and the Loess Plateau, which implied that an increase in vegetation coverage will increase the evaporation ratio (E/P) and reduce runoff ratio (R/P, where R is the long-term average runoff of the catchment) in these regions. This has been reported by several previous studies [*McVicar et al.*, 2007]. The negative correlation of $M \sim E/P$ found mainly in the Hai River basin implied that an increase in vegetation coverage will reduce the evaporation ratio (E/P) and increase runoff ratio (R/P) in this basin. However, this needs further validation from future field observations.

[26] On the Budyko curves shown in Figure 6, the positive correlation of $M \sim E/P$ indicated a positive correlation between n and M, which was true in the Yellow River basin and in the Inland River basin. The negative correlation of $M \sim E/P$ indicated a negative correlation between n and M, which was true in the Hai River basin. Since it was found that the forest land area fraction increases with the vegetation coverage in the study areas, the positive correlation between n and M was consistent with the Zhang's curves [*Zhang et al.*, 1999, 2001]; however, the negative correlation of $n \sim M$ suggested an opposite relationship. The inside mechanism causing the negative correlation of $M \sim E/P$ might be the nonlinear relationship between the actual evapotranspiration E and precipitation P in the catchment water balance equation resulting from the complex climate–vegetation–water cycle interactions.

4. Improving Water Balance Estimation by Incorporating the Vegetation Coverage

[27] From the above analysis, it is possible to improve the estimation of regional water balance by incorporating vegetation status into the Budyko curve. In fact, *Zhang et al.* [2001] has introduced different parameters for different vegetation types and calculated the catchment total long-term mean evapotranspiration for different vegetation types according to their area fractions. However, there was no consideration of vegetation coverage and its interannual variability in the water balance model in *Zhang et al.* [2001]. The present study used the regional water balance equation equation (3) to estimate annual water balance at the catchment scale. On the basis of the previous work by *Yang et al.* [2007], we attempted to incorporate vegetation coverage into the formulae for estimating the landscape

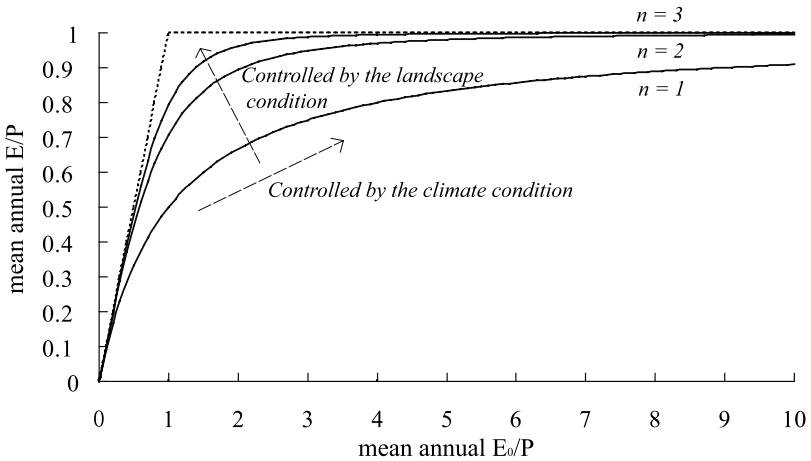

Figure 6. Interpreting complex interactions among climate, vegetation, and water balance by using the Budyko curves calculated by equation (3).

Table 7. Results of Stepwise Regression for Estimating the Landscape Parameter n[a]

	F	$F_{\alpha=0.05}$	r^2	Model Coefficients b_1	c_1	d_1	ln a_1
			$K_s/\overline{i_r}$				
Yellow River	47.1	4.0	0.413	−0.524	-	-	1.356
Hai River	6.4	4.2	0.187	−0.309	-	-	1.344
			$K_s/\overline{i_r}$, M				
Yellow River	38.2	3.1	0.536	−0.493	0.271	-	1.718
Hai River	5.0	3.3	0.270	−0.318	−0.228	-	1.125
			$K_s/\overline{i_r}$, M, tan β				
Yellow River	28.5	2.7	0.568	−0.368	0.292	−5.428	1.750
Hai River	4.1	2.9	0.320	−0.393	−0.301	4.351	1.001

[a]All of the parameters pass the F test with significance level of 1%; ln a_1 is the constant term; b_1, c_1, and d_1 are the parameters for the $K_s/\overline{i_r}$, M and tan β, respectively.

parameter n and for evaluating its impact on the interannual variability of catchment water balance.

[28] By using the long-term average annual precipitation, the potential evaporation, and actual evapotranspiration, the values of parameter n for the 99 study catchments were derived (see Table 1). We used the vegetation coverage (M) to replace the relative soil water storage ($S_{max}/\overline{E_0}$) recommended by *Yang et al.* [2007], where S_{max} is the plant extractable water capacity (see *Yang et al.* [2007] for more details), since both of M and $S_{max}/\overline{E_0}$ try to denote the vegetation information as one of the landscape factors and moreover M performs better than $S_{max}/\overline{E_0}$ in the stepwise regression. Since the opposite correlation of $M \sim n$ was found in the Hai River basin compared with the other study areas, all the catchments are separated into two groups: (1) the Hai River basin and (2) the Yellow River basin and the Inland River basin. Three nondimensional parameters, the relative infiltration capacity K_s/i_r, vegetation coverage M, and the average slope β are used to estimate the landscape parameter n in equation (3) by using the stepwise regression method (see Table 7), and the resulting empirical formulae of parameter n is given for the Yellow River basin and the Inland River basin as

$$n = 5.755\left(\frac{K_s}{\overline{i_r}}\right)^{-0.368} M^{0.292}\exp(-5.428\tan\beta) \qquad (6a)$$

and for the Hai River basin as

$$n = 2.721\left(\frac{K_s}{\overline{i_r}}\right)^{-0.393} M^{-0.301}\exp(4.351\tan\beta), \qquad (6b)$$

where $Ks/\overline{i_r}$ represents the relative infiltration capacity of the catchment, and tan β indicates the average slope of the catchment. Ks is the saturated hydraulic conductivity (mm h^{-1}), and $\overline{i_r}$ is the mean precipitation intensity (mm h^{-1}) in 24 hours (see *Yang et al.* [2007] for more details). By using equations (3) and (6), the long-term average actual evapotranspiration was obtained for the 99 catchments, and the results are plotted in Figure 7. The actual evapotranspiration obtained from equations (3) and (6) showed remarkable agreement with that derived from the long-term water balance with the determining coefficient of R^2 = 0.959 and the root-mean-square error (RMSE) of 21.87 mm.

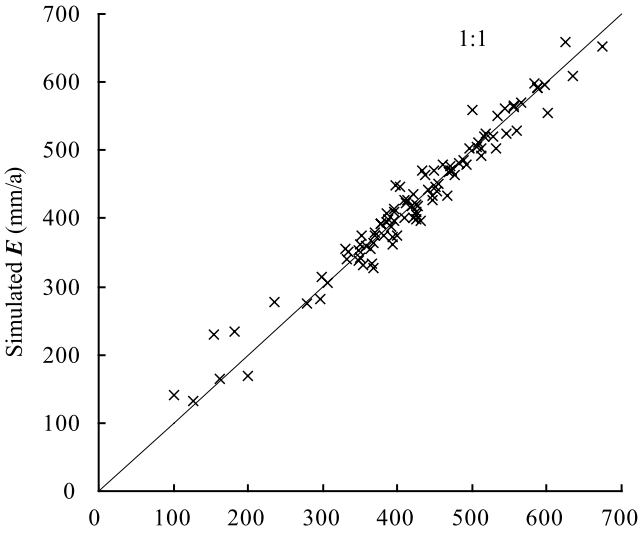

Figure 7. Comparing the long-term average annual evapotranspiration estimated by using equations (3) and (5) with that derived from water balance in the 99 study catchments.

[29] This model was also applied to evaluate the impact of the change in vegetation coverage on the interannual variability of the catchment water balance. The following two cases were considered for comparison: (1) using a constant n estimated from the long-term average vegetation coverage and (2) using a variable n estimated from the annual vegetation coverage. Figure 8 plots the comparison of the predicted actual evapotranspiration from these two cases for four selected catchments. The results indicated that the predicted actual evapotranspiration, based on equations (3) and (6) with a variable n, is better than that predicted by using a constant n, and both predictions had close agreement with the actual evapotranspiration derived from the observed data.

5. Conclusions

[30] The present study analyzed the impacts of vegetation on the regional water balance in the 99 catchments of northern China on the basis of the framework of the Budyko hypothesis. The following important conclusions can be drawn from this study;

[31] 1. From the vegetation distribution on the Budyko curves it is found that the annual average vegetation coverage (M) is mainly determined by the annual precipitation in the

Figure 8. Comparing the actual evapotranspiration estimated by using equations (3) and (5) with the constant parameter n (simulation 1) and variable n (simulation 2) with that estimated from water balance in four selected catchments. (a) catchment 4215 in the inland river basin, (b) catchment 42212 in the Yellow river basin, (c) catchment 44143 in the Yellow River basin, and (d) catchment 31551 in the Hai River basin.

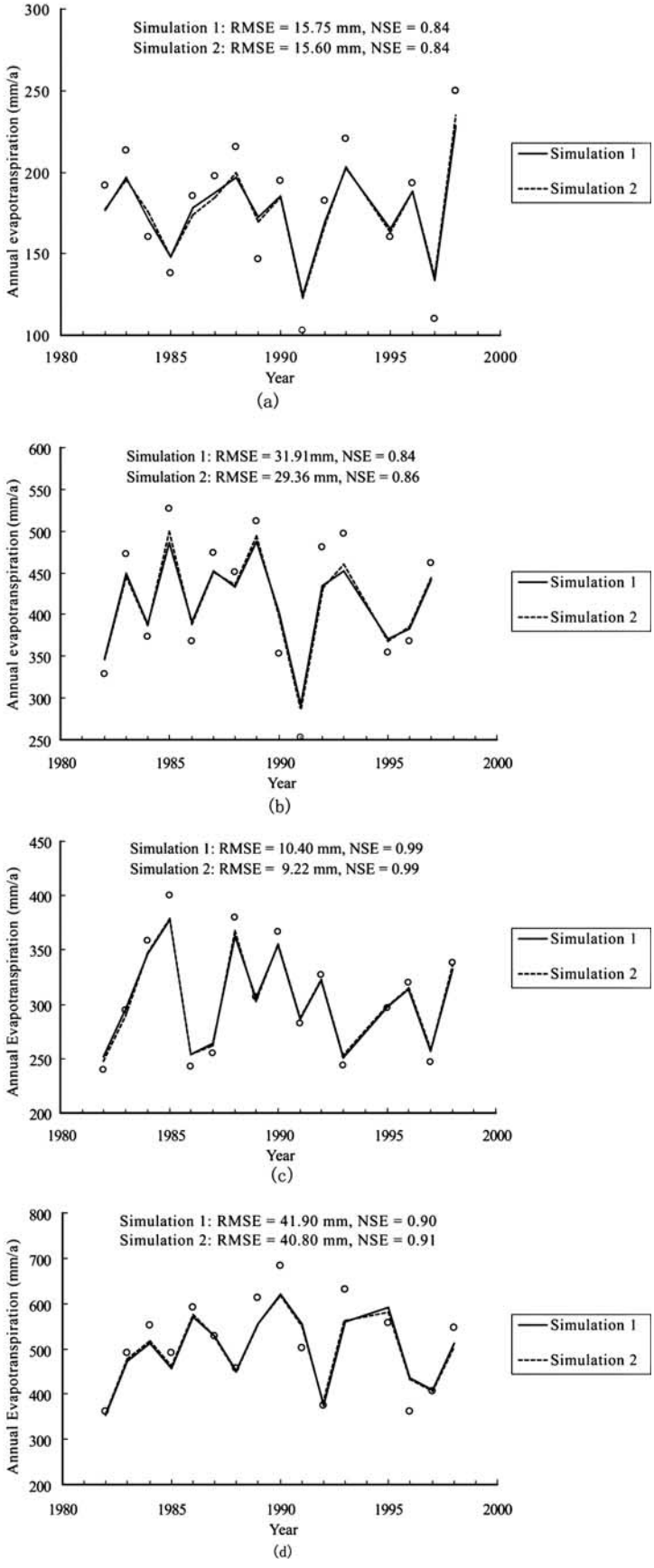
Simulation 1: RMSE = 15.75 mm, NSE = 0.84
Simulation 2: RMSE = 15.60 mm, NSE = 0.84
Annual evapotranspiration (mm/a)
Year
(a)
Simulation 1
Simulation 2
Simulation 1: RMSE = 31.91mm, NSE = 0.84
Simulation 2: RMSE = 29.36 mm, NSE = 0.86
Annual evapotranspiration (mm/a)
Year
(b)
Simulation 1
Simulation 2
Simulation 1: RMSE = 10.40 mm, NSE = 0.99
Simulation 2: RMSE = 9.22 mm, NSE = 0.99
Annual Evapotranspiration (mm/a)
Year
(c)
Simulation 1
Simulation 2
Simulation 1: RMSE = 41.90 mm, NSE = 0.90
Simulation 2: RMSE = 40.80 mm, NSE = 0.91
Annual Evapotranspiration (mm/a)
Year
(d)
Simulation 1
Simulation 2

Figure 8

nonhumid regions of China. In other words, the vegetation coverage in a relatively wetter environment (with higher P/E_0) tends to be denser and this leads to a higher evapotranspiration efficiency (E/E_0). However, it is found that the vegetation coverage also changes with landscape conditions even under a similar climate conditions, such as a similar dryness index.

[32] 2. In extremely dry or extremely wet environments, the regional annual water balance is controlled entirely by the climate with no relation to vegetation conditions. For normal climates, the regional water balance changes with both climate (dryness index) and landscape conditions, with the latter including the vegetation conditions represented by the parameter n in the coupled water–energy balance equation. However, the associated variability should not follow a single Budyko curve; instead it should cross different Budyko curves because of the interactions among vegetation, climate, and water cycle.

[33] 3. A positive correlation between the water balance component (E/P) and vegetation coverage (M) is found in most of the study catchments including the Yellow River basin and the Inland River basin. This implies that an increase in vegetation coverage may increase the evapotranspiration ratio (E/P) in these regions. However, a negative correlation of $M \sim E/P$ is also found in the Hai River basin, which implies that an increase in vegetation coverage may decrease the evapotranspiration ratio (E/P) there.

[34] 4. Vegetation coverage (M) is successfully incorporated into an empirical equation for estimating the landscape parameter n in the regional water–energy balance equation on the basis of the Budyko curve. It is found that the estimation of the interannual variability of regional water balance can be improved by considering the interannual variability of vegetation coverage.

[35] **Acknowledgments.** This research was supported by the joint research programs of the National Nature Science Foundation of China (NSFC, project 50721140161) and Japan Science and Technology (JST). The authors express their appreciation to Murugesu Sivapalan and to two anonymous reviewers, whose comments and suggestions led to significant improvements over the original manuscript.

References

Allen, R., L. Pereira, D. Raes, and M. Smith (1998), Crop evapotranspiration guidelines for computing crop water requirements, *FAO Irrig. Drain. Pap. 56*, Food and Agric. Organ. of the U. N., Rome.

Baudena, M., G. Boni, L. Ferraris, J. von Hardenberg, and A. Probenzale (2007), Vegetation response to rainfall intermittency in drylands: Results from a simple ecohydrological box model, *Adv. Water Resour.*, *30*(5), 1320–1328, doi:10.1016/j.advwatres.2006.11.006.

Bonan, G. B. (2002), *Ecological Climatology*, pp. 240–400, Cambridge Univ. Press, New York.

Brown, A. E., L. Zhang, T. A. Mamahon, A. W. Western, and R. A. Vertessy (2005), A review of paired catchment studies for determining changes in water yield resulting from alternations in vegetation, *J. Hydrol.*, *310*, 28–61, doi:10.1016/j.jhydrol.2004.12.010.

Budyko, M. I. (1974), *Climate and Life*, transl. from Russian by D. H. Miller, Academic, San Diego, Calif.

Carlson, T. N., and D. A. Ripley (1997), On the relation between NDVI, fractional vegetation cover, and leaf area index, *Remote Sens. Environ.*, *62*, 241–252, doi:10.1016/S0034-4257(97)00104-1.

Chen, L., Z. Huang, J. Gong, B. Fu, and Y. Huang (2007), The effect of land cover/vegetation on soil water dynamic in the hilly area of the loess plateau, China, *Catena*, *70*, 200–208, doi:10.1016/j.catena.2006.08.007.

Choudhury, B. J. (1999), Evaluation of an equation for annual evaporation using field observations and results from a biophysical model, *J. Hydrol.*, *216*, 99–110, doi:10.1016/S0022-1694(98)00293-5.

Cosandey, C., V. Andréassian, C. Martin, J. F. Didon-Lescot, J. Lavabre, N. Folton, N. Mathys, and D. Richard (2005), The hydrological impact of the Mediterranean forest: A review of French research, *J. Hydrol.*, *301*, 235–249, doi:10.1016/j.jhydrol.2004.06.040.

Donohue, R. J., M. L. Roderick, and T. R. McVicar (2007), On the importance of including vegetation dynamics in Budyko's hydrological model, *Hydrol. Earth Syst. Sci.*, *11*(2), 983–995.

Eagleson, P. S. (2002), *Ecohydrology: Darwinian Expression of Vegetation Form and Function*, pp. 170–207, Cambridge Univ. Press, New York.

Gutman, G., and A. Ignatov (1998), The derivation of the green vegetation fraction from NOAA/AVHRR data for use in numerical weather prediction models, *Int. J. Remote Sens.*, *19*, 1533–1543, doi:10.1080/014311698215333.

Holdridge, L. (1967), *Life Zone Ecology*, Trop. Sci. Cent., San Jose, Costa Rica.

Jiao, J., J. Tzanopoulos, P. Xofis, W. Bai, X. Ma, and J. Mitchley (2007), Can the study of natural vegetation succession assist in the control of soil erosion on abandoned croplands on the Loess Plateau, China, *Restor. Ecol.*, *15*(3), 391–399, doi:10.1111/j.1526-100X.2007.00235.x.

Laio, F., A. Porporato, L. Ridolfi, and I. Rodríguez-Iturbe (2001), Plants in water-controlled ecosystems: Active role in hydrologic processes and response to water stress: II. Probabilistic soil moisture dynamics, *Adv. Water Resour.*, *24*(7), 707–723, doi:10.1016/S0309-1708(01)00005-7.

Liu, J., M. Liu, X. Deng, D. Zhuang, Z. Zhang, and D. Luo (2002), The land use and land cover change database and its relative studies in China, *J. Geogr. Sci.*, *12*(3), 275–282, doi:10.1007/BF02837545.

McVicar, T. R., et al. (2007), Developing a decision support tool for China's re-vegetation program: Simulating regional impacts of afforestation on average streamflow in the Loess Plateau, *For. Ecol. Manage.*, doi:10.1016/j.foreco.2007.06.025.

Montandon, L. M., and E. E. Small (2008), The impact of soil reflectance on the quantification of the green vegetation fraction from NDVI, *Remote Sens. Environ.*, *112*, 1835–1845, doi:10.1016/j.rse.2007.09.007.

Oudin, L., V. Andréassian, J. Lerat, and C. Michel (2008), Has land cover a significant impact on mean annual streamflow? An international assessment using 1508 catchments, *J. Hydrol.*, *357*, 303–313, doi:10.1016/j.hydrol.2008.05.021.

Pike, J. G. (1964), The estimation of annual run-off from meteorological data in a tropical climate, *J. Hydrol.*, *2*, 116–123, doi:10.1016/0022-1694(64)90022-8.

Potter, N., L. Zhang, P. Milly, T. Mcmahon, and A. Jakeman (2005), Effects of rainfall seasonality and soil moisture capacity on mean annual water balance for Australian catchments, *Water Resour. Res.*, *41*, W06007, doi:10.1029/2004WR003697.

Rodríguez-Iturbe, I., and A. Porporato (2004), *Ecohydrology of Water-Controlled Ecosystems: Soil Moisture and Plant Dynamics*, Cambridge Univ. Press, New York.

Rodríguez-Iturbe, I., A. Porporato, F. Laio, and L. Ridolfi (2001), Plants in water-controlled ecosystems: Active role in hydrologic processes and response to water stress: I. Scope and general outline, *Adv. Water Resour.*, *24*(7), 695–705, doi:10.1016/S0309-1708(01)00004-5.

Shuttleworth, W. J. (1993), Evaporation, in *Handbook of Hydrology*, edited by D. R. Maidment, pp. 4.1–4.53, McGraw-Hill, New York.

Steven, M. D., T. J. Malthus, F. Baret, H. Xu, and M. J. Chopping (2003), Intercalibration of vegetation indices from different sensor systems, *Remote Sens. Environ.*, *88*, 412–422, doi:10.1016/j.rse.2003.08.010.

Xu, X., H. Zhang, and O. Zhang (2004), Development of check-dam systems in gullies on the Loess Plateau, China, *Environ. Sci. Policy*, *7*, 79–86, doi:10.1016/j.envsci.2003.12.002.

Xu, X., G. Ding, B. Sun, M. Zhao, and H. Jin (2007), Ecological water requirement of major sand shifting control forest in Minqin oasis of lower researches of inland river (in Chinese), *J. Soil Water Conserv.*, *21*(3), 144–148.

Yang, D., C. Li, H. Hu, Z. Lei, S. Yang, T. Kusuda, T. Koike, and K. Musiake (2004), Analysis of water resources variability in the Yellow River of China during the last half century using historical data, *Water Resour. Res.*, *40*, W06502, doi:10.1029/2003WR002763.

Yang, D., F. Sun, Z. Liu, Z. Cong, and Z. Lei (2006), Interpreting the complementary relationship in non-humid environments based on the Budyko and Penman hypotheses, *Geophys. Res. Lett.*, *33*, L18402, doi:10.1029/2006GL027657.

Yang, D., F. Sun, Z. Liu, Z. Cong, G. Ni, and Z. Lei (2007), Analyzing spatial and temporal variability of annual water-energy balance in nonhumid regions of China using the Budyko hypothesis, *Water Resour. Res.*, *43*, W04426, doi:10.1029/2006WR005224.

Yang, H., D. Yang, Z. Lei, and F. Sun (2008a), New analytical derivation of the mean annual water-energy balance equation, *Water Resour. Res.*, *44*, W03410, doi:10.1029/2007WR006135.

Yang, H., D. Yang, Z. Lei, and H. Lei (2008b), Derivation and verification of the coupled water-energy balance equation at arbitrary time scale (in Chinese), *J. Hydraul. Eng.*, *39*(5), 610–617.

Zeng, X., X. Zeng, S. Shen, R. Dickinson, and Q. Zeng (2005), Vegetation-soil water interaction within a dynamical ecosystem model of grassland in semi-arid areas, *Tellus, Ser. B*, *57*, 189–202.

Zhang, L., W. R. Dawes, and G. R. Walker (1999), Predicting the effect of vegetation changes on catchment average water balance, *Tech. Rep. 99/12*, CRC for Catchment Hydrol., Canberra.

Zhang, L., W. R. Dawes, and G. R. Walker (2001), Response of mean annual evapotranspiration to vegetation changes at catchment scale, *Water Resour. Res.*, *37*(3), 701–708, doi:10.1029/2000WR900325.

Zhang, L., K. Hickel, W. R. Dawes, F. H. S. Chiew, A. W. Westem, and P. R. Briggs (2004), A rational function approach for estimating mean annual evapotranspiration, *Water Resour. Res.*, *40*, W02502, doi:10.1029/2003WR002710.

Zhang, X., L. Zhang, T. R. McVicar, T. G. Van Niel, L. Li, R. Li, Q. Yang, and L. Wei (2007), Modelling the impact of afforestation on average annual streamflow in the Loess Plateau, *China, Hydrol. Processes*, *22*, 1996–2004, doi:10.1002/hyp.6784.

W. Shao, D. Yang, and H. Yang, State Key Laboratory of Hydro-Science and Engineering, Department of Hydraulic Engineering, Tsinghua University, Beijing 100084, China. (yangdw@tsinghua.edu.cn)

S. Kanae, T. Oki, and P. J.-F. Yeh, Institute of Industrial Science, University of Tokyo, 4-6-1 Komaba, Meguro-ku, Tokyo, 153-8505, Japan.